# EXPERIMENTAL STUDY OF AEROSOL DISPERSION IN A SINGLE-AISLE AIRCRAFT WITH CABIN DISPLACEMENT VENTILATION

T. Dehne, A. Volkmann, D. Schmeling, German Aerospace Center (DLR), Institute of Aerodynamics and Flow Technology, Bunsenstraße 10, 37073 Göttingen, Germany

#### Abstract

Novel ventilation systems for aircraft cabins have attracted the attention of scientists and aircraft manufacturers over the last years due to their potential in terms of energy saving and generating a higher level of thermal comfort. Since the coronavirus pandemic the spread of aerosol particles in cabins has become another important criterion. Recent studies based on computational fluid dynamics simulations highlight the advantages of cabin displacement ventilation (CDV): reduced spreading of aerosol particles in the cabin and faster as well as enhanced particle removal.

The aim of the present study is to experimentally determine the aerosol dispersion of state-of-the-art mixing ventilation (MV) — currently installed in almost all commercial aircraft — and of CDV in the Do 728 test facility of the German Aerospace Center in Göttingen. Both concepts were analyzed in terms of various airflow rates. Further, the location of the index passenger was varied in spanwise and longitudinal direction to allow for a detailed analysis and to improve the fundamental knowledge on the parameters determining the aerosol dispersion.

Overall, the results of the present study expand the knowledge regarding the influence of passenger cabin ventilation on the spread of aerosol particles. The main result is a wider distribution under mixed ventilation conditions as well as higher concentrations due to forced convection, while cabin displacement ventilation shows a much better removal of the aerosol particles. Further, the mean and maximum aerosol concentrations are lower for CDV compared to MV conditions. In case of MV, the spread of particle is strongly influenced by the source position, both longitudinally and in the cross-section direction.

#### **Keywords**

Aircraft cabin, mixing ventilation, cabin displacement ventilation, aerosol dispersion, COVID-19

### 1. INTRODUCTION

Since the start of the COVID-19 pandemic in 2020 and the associated discussions about the spread of viruses, many studies have shown that the absorption of aerosol particles through the mucous membranes plays a major role in the spread of the coronavirus [1], [2]. Aerosol particles between 0.1 µm and 10 µm have been identified to have an increased probability of transmission as they can be more easily distributed by the airflow in the room [3]. An older study shows that 80% of the particles in the human breath are smaller than 1 µm and 99% are smaller than 5 µm [4]. Effective measures to ensure high air quality standards with regard to air pollution and the potential viral load in current aircraft ventilation systems are high air flow rates in the cabin and high-efficiency particulate air filters (HEPA) [5], [6]. The mixing ventilation system (MV) installed in aircraft cabins achieves a strong mixing of the cabin air with the fresh air through high air supply velocities. This guarantees the desired stable conditions, which, however, potentially increases the transport of particles from one passenger to another [7]. Based on numerical tracer gas analyses, the study shows improved efficiency with personalized displacement ventilation in 7-row cabin models. Aerosol dispersion using the so-called Lagrangian particle transport analysis was investigated by means of CFD simulations for three different configurations in a Boeing 737 under MV conditions [8]. An increased particle concentration in a localized area of plus/minus two rows around the index passenger was found.

For the experimental analysis of ventilation systems in longrange aircraft, a modern two-aisle cabin model was developed at the German Aerospace Center (DLR) in Göttingen using original interior parts [9]. MV and alternative ventilation systems were investigated with regard to passenger thermal comfort and energy efficiency, considering, e.g., different boundary conditions or the influence of unoccupied seats. The results of the alternative ventilation systems were compared with the MV reference scenarios [9], [10], [11], highlighting the advantages and disadvantages of the different ventilation concepts in terms of thermal comfort and energy efficiency. For cabin displacement ventilation (CDV) an alternative ventilation concept is introduced: the fresh air is supplied through the floor with very low momentum. It rises near the heat loads due to buoyancy and leaves the cabin in the ceiling area. This leads to a high heat and aerosol removal efficiency. CDV has been studied for several years in numerical simulations, ground-based facilities and even under flight conditions, see e.g., [12], [13], [14], [15], [16]. In a recent study in the above-mentioned two-aisle aircraft cabin mockup [17], special attention was paid to aerosol particle dispersion. The dispersion of particles, exhaled by an "index" passenger, was experimentally investigated using thermal manikins and many particulate matter sensors. The spread of particles is strongly influenced by the ventilation system, where MV showed a stronger mixing of the exhaled aerosol particles in the cabin. In contrast, the aerosol spreading was greatly reduced in case of CDV. However, a seat with highly increased concentrations was always found near the "index" passenger for CDV. The mean aerosol concentration is more than 50% lower for CDV compared to MV, while the maximum concentration for CDV is six times higher than for MV. Furthermore, it was found that the spread of particles is strongly influenced by the position of the particle source.

Another test environment at the DLR in Göttingen is the Dornier Do 728. It offers the possibility to perform measurements in a real aircraft without certification effort. MV and alternative ventilation systems were investigated in this facility with respect to passenger thermal comfort and efficiency, but also in terms of the impact of unoccupied seats [15], [18]. Furthermore, another experimental and numerical study shows the positive effect of wearing a mask and applying an increased airflow. Especially the combination of both factors was investigated [19].

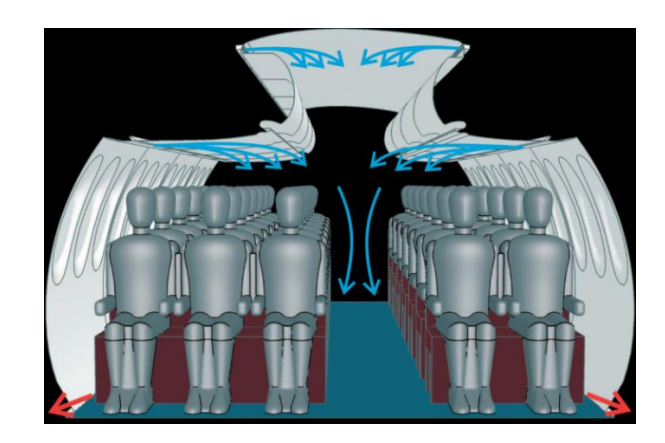
The present experimental study focusses on the spreading of aerosol particles from one source, the "index" passenger, for MV and CDV in the test environment Do 728 using an aerosol-exhaling thermal manikin. The first aim of this study is to expand the knowledge on the influence of the state-of-the-art ventilation (MV) concept used for the passenger cabins on the dispersion of aerosol particles. Therefore, we experimentally determine the aerosol dispersion in longitudinal as well as cross-sectional direction. As a second objective, the numerically predicted advantages of CDV over MV in terms of particle spreading will be experimentally determined.

## 2. TEST ENVIRONMENT AND VENTILATION SYSTEM

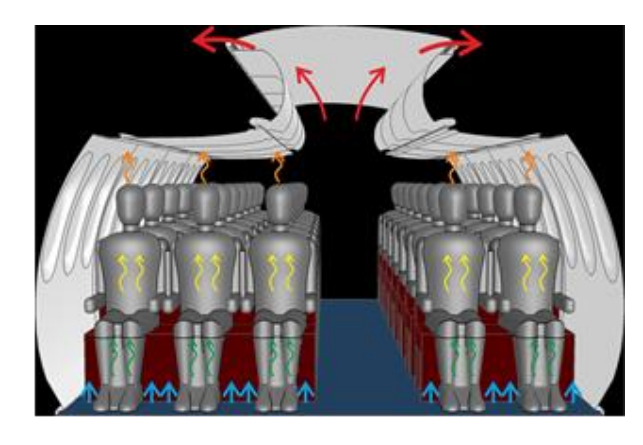
As test environment, the Do 728 test facility of the German Aerospace Center in Göttingen was used. It provides a realistic cabin structure of a short-range aircraft cabin. FIG 1 (a) depicts a cross section of the asymmetric single-aisle cabin which has a total length of 16.9 m, a width of 3.25 m and a height of 2.14 m. The free air volume within the cabin, i.e., inner volume without seats and thermal manikins, amounts to approx. 54 m<sup>3</sup>. An external heating, ventilation and air-conditioning (HVAC) system provided fresh air at a nominal volume flow rate of  $Q_V = 600 \text{ l/s}$  (8.2 l/s/PAX) at atmospheric pressure yielding a nominal air exchange rate of 38 air changes per hour (ACH). Mixing ventilation (MV) was operated at a half-half split of the air flow between lateral (LAO) and ceiling air outlets (CAO). As the research aircraft is designed with a 2-3 seating arrangement, see FIG 1 (b), the air supply to the passengers was split as follows: 40% from the left and 60% from the right. Thus, the distribution was 20% left LAO, 20% left CAO, 30% right LAO and 30% right CAO. Please note: orientations such as left and right refer to the direction of flight, whereas the images and sketches in FIG 1 face the rear of the cabin. The air was supplied with nominal mean entry velocities of 1.7 m/s into the cabin and the resulting air jets ensured efficient mixing of fresh and recirculated air and generated the large-scale roll structures, which are characteristic for MV as indicated in FIG 1 (b). The air was removed from the cabin by active suction through air extraction slits behind the dado panels located in the lower side walls. The alternative cabin displacement ventilation (CDV) system is based on the supply of fresh air in the floor area, see FIG 1 (c). The fresh air - introduced with low momentum - rises due to buoyancy near the heat loads and leaves the cabin in the crown area through the ceiling outlets above the side luggage compartments. The supply air volume flow was split in a similar way as MV: a 40% - 60% distribution of the supply air for the 2-3 seating arrangement was realized. CDV has been shown to offer a significantly higher heat removal efficiency at very low flow velocities compared to MV. However, the CDV systems described in the literature so far tend to create potentially uncomfortable temperature stratification. Therefore, the fresh air was increased to a nominal volume flow rate of 700 l/s (10 l/s/PAX) for this study.



(a)



(b)



(c)

FIG 1. (a) Image of the interior of the Do 728 as well as ventilation systems in (b) Mixing ventilation (MV) and (c) cabin displacement ventilation (CDV).

### 3. MEASUREMENT TECHNIQUES AND TEST CASES

This section briefly describes the measuring techniques used to determine the aerosol distribution and the necessary boundary conditions. For a realistic heat load and to simulate the dimensions of real people, thermal manikins (TMs) with a volume of 0.05 m<sup>3</sup> and a surface of 1.52 m<sup>2</sup> were used in the experimental investigations, see FIG 2 (a). The TMs were operated at a constant heat release rate of 75 W. The cabin measurement installation basically comprises sensor racks with resistance temperature detectors (RTDs) to calculate the mean cabin air temperature T<sub>cab</sub> at four height levels (ankle, knee, chest, head) close to the TMs at a distance of 5 cm in rows 4, 8 and 12, see FIG 2 (b). Furthermore, FIG 2 (b) shows the sensors installed for the supply (Tin) and exhaust (Tout) air under MV and CDV conditions, also in rows 4, 8 and 12. It has to be noted that  $T_{\text{cab}}$  serves as a control temperature and was kept constant during the steady-state conditions. To reach the setpoint and to keep it constant, Tin was adjusted individually for each of the studied cases.



Flight direction

(a)

(b)

FIG 2. (a) Photo of the installed measurement systems in the cabin including the aerosol source (face) and the particulate matter sensors (green boxes at the heads). (b) Cabin layout and measurement installation in the Do 728. The temperature probes near the TMs and in the supply and exhaust air are marked with blue and magenta squares, respectively. Further, the positions of the particulate sensors in front of the TMs (green squares) as well as nine different source positions, i.e., seats of the index passenger, (red circles) are indicated.

An aerosol generator with an airbrush pistol (AFC-101A, nozzle diameter 0.35 mm) was used to generate and distribute the aerosol particles (artificial saliva - mixed in

accordance with NRF 7.5) [20]. After completion of the evaporation process (using an atomization and settling chamber with a pipe system), only pure, dry particles with sizes between 0.3 and 2.5 µm were released, with a peak number concentration occurring at a size of approx. 0.8 µm. To ensure realistic mouth-nose exhalation and to control the exhaust air volume flow, the system was connected to a face mask (FIG 2 a) and a volume flow sensor. The aerosol source produced much higher particle concentrations compared to normal human exhalation to allow for a better signal to noise ratio and to allow for the use of our low-cost sensor data acquisition system, see next paragraph. The key data of the aerosol source are also summarized in [19].

Low-cost particulate matter sensors (SPS30 [21]) were used for the spatially resolved detection of particle number densities inside the cabin. A pre-calibration in a sealed box using an OPS probe [24] confirmed the accuracy of the SPS30 sensors as indicated by the manufacturer, i.e., error 10% of the measured value or 20/cm3 - whichever is greater, for two size bins (0.3 - 1.0 µm and 1.0 - 2.5 µm), In our measurements, 70 SPS30 sensors were positioned at the faces of the TMs (see FIG 2 (a) and (b)) and recorded the local aerosol particle concentrations in the breathing zone of each passenger at a rate of 0.9 Hz. The aerosol concentration, averaged over 300 s, was calculated at stationary conditions to account for short-time fluctuations of the local concentrations. Afterwards, the locally measured averaged equilibrium particle concentration was multiplied by the typical human tidal volume (600 ml/breath) and the typical respiratory rate of 10 breaths per minute. This gives the amount of measured "inhaled" particles per minute. As described above, we operated the aerosol source at an increased particle production rate compared to normal human exhalation. Therefore, in a further step, the inhaled aerosols [particles/minute] were divided by the produced aerosols [particles/minute], which gives the number of inhalation fraction  $f_N = \frac{N_{seat}}{N_{source}}$ . In other words,  $f_N$  determines the percentage amount of all exhaled particles that are inhaled at a specific location.

### 4. RESULTS

3

FIG 3 exemplarily shows the aerosol dispersion for the source position 6C, marked by the black letter "S", for stateof-the-art MV with "Norm-Flow" Qv = 600 l/s. The color bar was chosen to resolve differences for lower concentrations. However, it should be noted that the peak aerosol concentrations were higher than the maximum value of the color bar. The absolute values of the peak aerosol concentrations, in terms of the peak inhalation fraction, can be found in the respective tables in the following subsections. The results shown in the figure reveal that the highest concentrations can be found on the other seats in the row of the source and one row in front. Thereby, the highest values are recorded on the same side as the source, However, the inhalation fraction on the other side of the aisle is also significantly increased compared to the seat farther away from the source. Only rather low values below approx. 0.05% are recorded on all seats more than two rows away from the source.

©2024

These findings can be explained by the flow pattern of the MV system: The flow is mainly two-dimensional, i.e., most particles are transported within the same row. However, it has also non-neglectable components in longitudinal direction, which result in the spreading of the exhaled aerosol particles to the other rows. The exhaled particles rise in the vicinity of the heated thermal manikin, then the forced airflow generated by the LAOs transports the particles towards the aisle region. The downwash in the aisle region – caused by the superposition of the airflow of both LAOs and CAOs – transports the particles towards the floor. The flow separates towards both sides and partly recirculates due to the thermal convection close to the passengers and partly leaves the cabin through the air outlets, see also sketch in FIG 1 (b).

Due to the high flow velocities and the resulting high forced convection, the aerosol particles are distributed quite broadly in the cross-section and in two rows in front and behind the source.

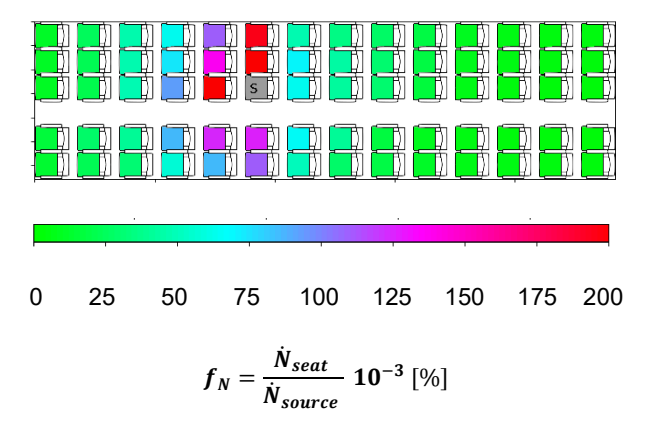


FIG 3. Spatial distribution of steady-state inhalation fraction at MV with  $Q_V$  = 600 l/s and the source "S" on seat 6C.

After this brief general discussion of the spreading from one exemplary seat, the following sections contain the detailed discussion of the results: Chapter 4.1 describes the results for a varied source position at a standard volume flow QV = 600 l/s on 5 seats (A, B, C, D, E) in cross section in row 6. The following chapter deals with the aerosol propagation from five different source positions in longitudinal direction (seats 4, 5, 6, 7, 8) in column C.

Further, chapter 4.3 shows a comparison of the different ventilation systems at a standard volume flow (MV - 600 l/s and CDV - 700 l/s). Finally, in chapter 4.4, two extreme conditions "High-Flow" for MV (800 l/s) and "Low-Flow" for CDV (300 l/s) are compared.

### 4.1. Influence of different source locations in cross section for MV

FIG 4 shows the local inhalation fractions, i.e., the normalized particle concentrations under MV conditions for five different source locations. In accordance with one of the main results that no significantly increased inhalation fractions were found more than two rows away from the source (see FIG 3) we cropped the result images for the

following cases to this selected region. Five different source locations within one fixed row, i.e., 6A to 6E, are shown in the five sub-figures. In addition, TAB 1 shows the maximum  $(f_N^{max})$  and the mean  $(f_N^{mean})$  aerosol concentration. Further, the number of seats with an inhalation fraction  $f_N > 0.03\%$ , > 0.06% and > 0.10% are indicated in TAB 1.

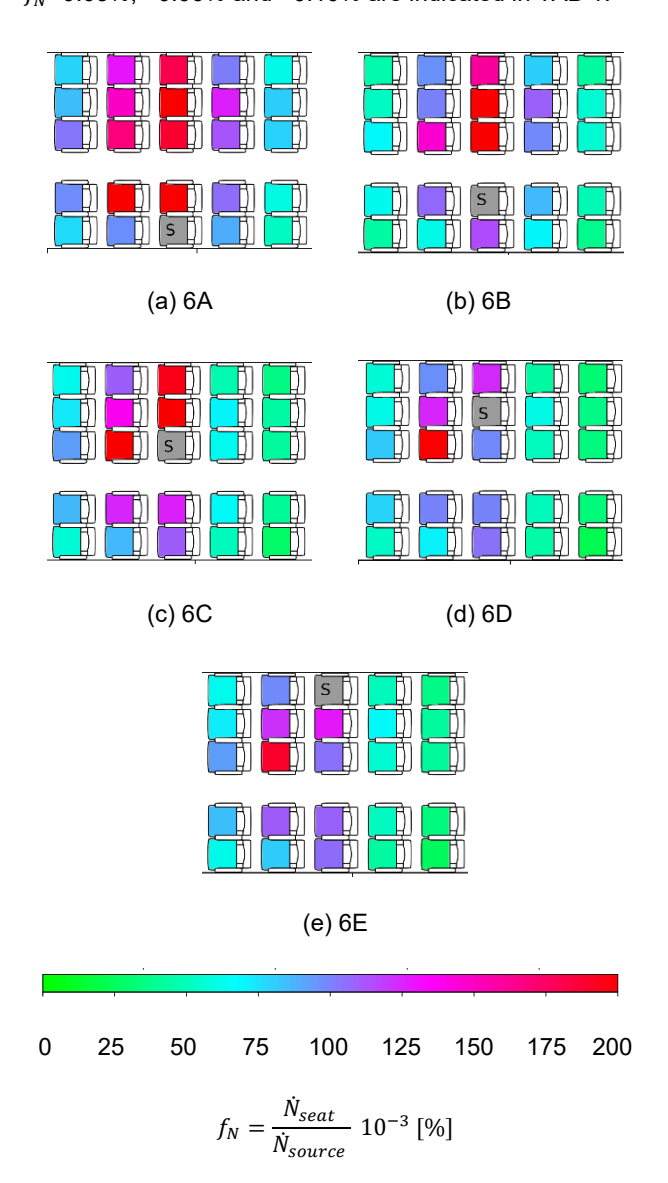


FIG 4. Spatial distribution of steady-state inhalation fraction at MV with  $Q_V$  = 600 l/s for five different source positions in row 6.

FIG 4 (a), i.e., source position on the left window seat (6A), shows strongly increased inhalation fractions in the whole row 6. The aerosol distribution for the seating positions 6B and 6C in (b) and (c) is similar. The highest aerosol concentration was found on the right neighboring seat: 0.26% for source 6A, 0.23% for 6B and 0.31% for source position 6C, see TAB 1. In contrast, for the source positioned on seats 6D and 6E, we found the peak concentration not within row six, but in the row in front of the source. Here, values up to  $f_N = 0.22\%$  were found for seat position 6D. Furthermore, the results reveal that the mean particle concentration on the 24 surrounding places (5 rows) decreases if the source moves from the left to the right, i.e., 6A to 6E, see also TAB 1. However, all results

show a rather wide distribution of the aerosol particles in the cabin, which means that values above 0.03% were also measured in flight direction left (FDL), whereas the source was located in flight direction right (FDR) and vice versa. In total, a local aerosol concentration higher than  $f_N = 0.03\%$ was detected at up to 40 seats for source position 6A, see TAB 1. Further, the highest number of seats with an aerosol concentration above 0.03%, 0.06% and 0.10% was found for seat 6A, see TAB 1. Apparently, a higher aerosol concentration occurs starting from the source positions 6A and 6B, whereas the aerosols are better removed from the cabin at the source positions in FDR. However, the highest value of  $f_N = 0.31$  was found for source position 6°C. No significant differences were found in the mean values, except for the highest value at source position 6A, which was almost twice as high as the lowest case (6D), see TAB 1.

From the observations discussed above, we can summarize that the particles propagate mainly within the row of the source. Further, the propagation towards the front is stronger than towards the rear. There is a significant difference of the particle spreading for different source locations within a row. This can be attributed to the flow pattern in the cabin, which is a result of the high inflow velocities.

TAB 1. Investigated cases of different source positions in cross section with maximum and mean number of the inhalation fraction including the number of seats with an inhalation fraction exceeding 0.03%, 0.06% and 0.10%.

	$f_N^{mean}$	$f_N^{max}$ [%]	Number of seats with $f_N$ >			
	[%]		0.03 [%]	0.06 [%]	0.10 [%]	
6A	0.06	0.26	40	24	13	
6B	0.04	0.23	32	17	8	
6C	0.04	0.31	29	17	9	
6D	0.03	0.22	28	14	5	
6E	0.04	0.19	29	16	8	

# 4.2. Influence of different source locations in longitudinal direction for MV

The airflow in aircraft cabins, however, is not purely two-dimensional, as already confirmed in previous studies [22]. To discuss these differences in longitudinal direction, FIG 5 shows the aerosol concentration in a selected region around the particle source for different sources in rows 4 – 8. The seat position C and the standard volume flow Qv = 600 l/s were kept constant for these comparisons. Additionally, TAB 2 shows the maximum  $(f_N^{max})$  and the mean  $(f_N^{mean})$  aerosol concentration as well as the number of seats with an inhalation fraction above the thresholds of 0.03%, 0.06% and 0.10%.

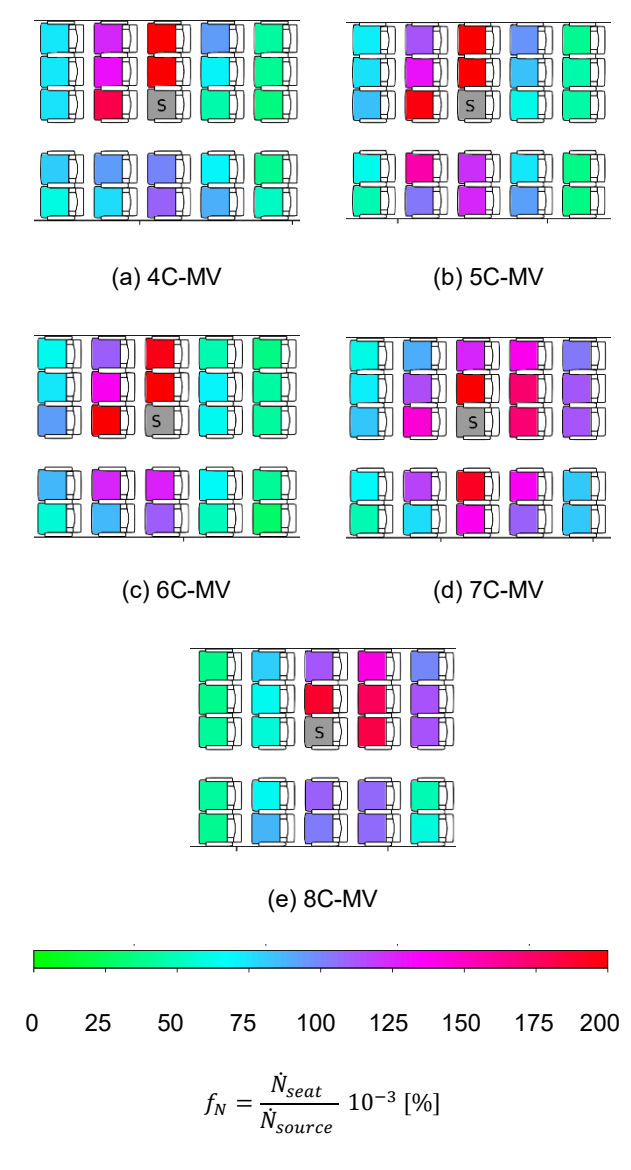


FIG 5. Spatial distribution of steady-state inhalation fraction for MV with  $Q_V = 600$  l/s for five different source positions in column C.

TAB 2. Investigated cases of different source positions in longitudinal direction with maximum and mean number of the inhalation fraction including the number of seats with an inhalation fraction exceeding 0.03%, 0.06% and 0.1%

	$f_N^{mean} = [\%]$	$f_N^{max}$ [%]	Number of seats with $f_N$ >			
			0.03 [%]	0.06 [%]	0.10 [%]	
4C	0.04	0.30	29	19	7	
5C	0.05	0.29	32	19	10	
6C	0.04	0.31	29	17	9	
7C	0.06	0.26	43	27	16	
8C	0.05	0.20	40	18	12	

Similar results are shown for source positions 4C, 5C and 6C (Fig a - c) with concentrations  $\geq 0.20\%$  on the adjacent seats D and E as well as on the front seat. The highest concentrations of 0.29% (5C), 0.30% (4C) and 0.31% (6C), see TAB 2, were found in the immediate vicinity of the source on the right neighboring seat. In comparison, lower aerosol concentrations of up to 0.13% were observed on the left side of the aisle. Further, the spread in the other rows is very similar. While the figure shows an aerosol concentration of 0.08% - 0.09% in the two rows in front of the source, slightly lower values of 0.04% - 0.05% were found in the rear area.

In contrast, a completely different aerosol distribution could be observed for source positions 7C in FIG 5 (d) and 8C in FIG 5 (e). With a maximum of 0.08% in row 5 for source position 7C and 0.04% in row 6 for source position 8C, the figures show a higher particle transport into the rear rows, which is reflected by maximum values of 0.11% two rows behind the source for both cases. The situation is similar in the directly adjacent rows. Here too, higher aerosol concentrations were measured in the row behind the source (maximum values 0.17% for 7C and 0.18% for 8C) compared to the row in front of it (0.14% for 7C and 0.08% for 8C). However, the aerosol distribution in cross section differed: while at source position 8C the by far highest concentration (0.19%) was measured to the right of the source, FIG 5 (d) shows equal value to the left and right of the source (0.19% each). The figures show that no uniform result could be obtained for the aerosol source position C. While the majority of particles are transported forward at source positions 4 - 6, from row 7 onwards they flow into the rear part of the cabin. This finding confirms the existence of three-dimensional flow pattern in an aircraft cabin.

### 4.3. Comparison of MV and CDV under "Norm-Flow" conditions

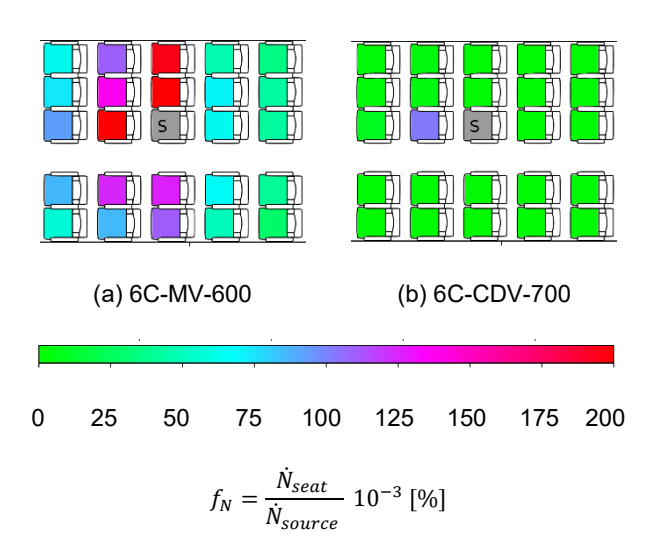


FIG 6. Spatial distribution of steady-state inhalation fraction for MV (a) and CDV (b) for source position 6C.

FIG 6 shows the aerosol concentration in the selected region around the particle source starting from seat position 6C for MV and CDV. The ventilation systems were compared under standard conditions, which means a volume flow of 600 l/s for MV (8.2 l/s/PAX) for MV (FIG 6 a)

and a slightly higher value of 700 l/s (10 l/s/PAX) for CDV, see FIG 6 (b). Under MV conditions the aerosol particles were distributed on two seats in all directions starting from source position 6C, for CDV only one increased value was found on seat 5C.

TAB 3. Comparison of MV on source positions 6C with CDV on nine seat positions with maximum and mean number of inhalation fraction as well as the number of seats with an inhalation fraction exceeding 0.03%, 0.06% and 0.1%.

exceeding 0.03%, 0.06% and 0.1%.						
	$f_N^{mean}$	$f_N^{max}$ [%]	Number of seats with $f_N$ >			
	[%]		0.03 [%]	0.06 [%]	0.10 [%]	
6C-MV-600	0.040	0.31	29	17	9	
6A-CDV-700	0.005	0.10	2	2	0	
6B-CDV-700	0.005	0.09	2	1	0	
4C-CDV-700	0.004	0.05	2	0	0	
5C-CDV-700	0.002	0.07	1	1	0	
6C-CDV-700	0.010	0.10	2	1	1	
7C-CDV-700	0.003	0.09	1	1	0	
8C-CDV-700	0.003	0.08	1	1	0	
6D-CDV-700	0.007	0.18	2	2	2	
6E-CDV-700	0.004	0.06	3	1	0	

For the comparison, TAB 3 summarizes the corresponding values  $f_N^{max}$  and  $f_N^{mean}$  as well as the number of seats with an inhalation fraction above the thresholds of 0.03%, 0.06% and 0.10%. Additional configurations of CDV are also included in the table. Due to space constraints and for the sake of brevity, the additional figures for CDV are not included in this paper. When comparing seating position 6C, MV reveals a maximum value of 0.31%, whereas CDV shows a value which is only one third of the MV peak value. Moreover, the maximum value (0.18%) found at source position 6D is 45% smaller for CDV. Based on the mean aerosol concentration, the measured value was reduced by 75% using CDV compared to MV. Concentrations larger than 0.03% were found under CDV conditions on three or less seats. The number of seats with an inhalation fraction above 0.06% and 0.1% is two or less at source position 6D. As already mentioned at the beginning and shown in FIG 6, CDV reveals great advantages when it comes to the removal of particles from the cabin through vertical ventilation which is once again demonstrated by the values in TAB 3.

### 4.4. Comparison of extreme conditions: Highflow for MV and Low-flow for CDV

Finally, a comparison of the ventilation systems with different volume flows was carried out to further highlight the advantages of CDV. For this purpose, we increased the flow rate for MV to decrease the contamination levels in the cabin. Simultaneously, we strongly decreased the flow rate for CDV to prove that the airflow pattern removes the particles even at low flow rates. FIG 7 (a) shows the results for MV with a flow rate increased by 1/3 ("High-Flow"  $Q_V = \frac{1}{2} \left( \frac{1}{2} \right) \left( \frac{1}{2} \left( \frac{1}{2} \right) \left( \frac{1}{2} \right) \left( \frac{1}{2} \left( \frac{1}{2} \right) \left( \frac{1}{2} \right) \left( \frac{1}{2} \right) \left( \frac{1}{2} \left( \frac{1}{2} \right) \left( \frac{1}{2} \right) \left( \frac{1}{2} \right) \left( \frac{1}{2} \right) \left( \frac{1}{2} \left( \frac{1}{2} \right) \left( \frac{1}{2} \right) \left( \frac{1}{2} \right) \left( \frac{1}{2} \right) \left( \frac{1}{2} \left( \frac{1}{2} \right) \left$ 

©2024

6

800 l/s). FIG 7 (b) shows CDV at a very low flow rate ("Low-Flow"  $Q_V = 300$  l/s). What is immediately noticeable at MV – despite the considerably higher volume flow – is that a significantly larger spreading around the source occurs. For CDV depicted in (b), a greater dispersion of particles was also observed due to the reduced volume flow, but mainly near the source. A comparison of the mean and maximum values indicated in TAB 4 shows the higher values for MV despite the supply air reduction for CDV and thus considerable energy savings. Furthermore, for MV there were more seats with increased aerosol concentrations above the thresholds of 0.03%, 0.06% and 0.10% for the source position 6C. However, FIG 7 also shows a farther distribution of particles throughout the cabin for CDV with values > 0.07% in row 1.

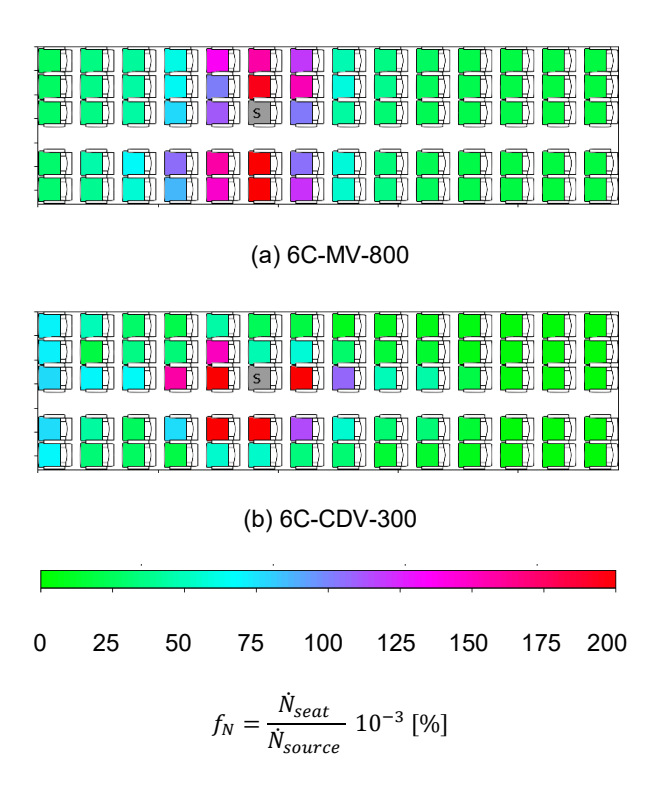


FIG 7. Spatial distribution of steady-state inhalation fraction for MV (a) and CDV (b) for source positions 6C.

TAB 4. Investigated cases of MV and CDV with different volume flows on seat position 6C with maximum and mean number of the inhalation fraction including the number of seats with an inhalation fraction exceeding 0.03%, 0.06% and 0.1%

	$f_N^{mean}$	JN	Number of seats with $f_N$ >		
	[%]	[%]	0.03 [%]	0.06 [%]	0.10 [%]
6C-MV-800	0.06	0.36	40	21	15
6C-CDV-300	0.04	0.26	32	16	8

### 5. DISCUSSION AND CONCLUSION

This paper presents the results of experimental investigations on the aerosol propagation using the Dornier 728 aircraft cabin test facility of the German Aerospace Center in Göttingen as test environment. To ensure realistic aerosol exhalation, artificial saliva was introduced into the cabin through a facial geometry with mouth and nose openings. At the same time 70 aerosol particle sensors enabled a spatially and temporally resolved analysis of the local aerosol particle concentrations in the inhalation zones of the other passengers, simulated by heated thermal Two ventilation systems were human manikins. investigated: first, mixing ventilation (MV) - state-of-the-art for ventilation of passenger aircraft - with high inflow velocities and thus a higher forced convection. Second, cabin displacement ventilation (CDV) with low inflow velocities at floor level.

Due to high inflow velocities in case of MV and the resulting increased forced convection, the aerosol particles are distributed in several rows. Mostly low particle concentrations were measured, with maximum values of 0.31%. However, the highest recorded concentration was not always in the immediate vicinity of the source, as shown by the maximum value on seat 5C for the source positions window (6E) and middle seat (6D). The source in the aisle in row 7 (seat C) leads to the greatest particle spread compared to all other source positions. Up to 43 seats were found with a contamination of  $f_{N} > 0.03\%$ . In contrast, source position 6D shows the lowest spread with 28 seats. Despite the high degree of mixing of fresh air with cabin air, MV shows up to 16 seats with values of  $f_{N} > 0.1\%$ .

Due to free convection in CDV, a lower dispersion of particles in the cabin was measured. Slightly elevated concentrations occurred mainly near the source, reflecting peak concentrations of up to 0.1% (source 6C). Furthermore, CDV shows a maximum of three seats with an aerosol concentration of  $f_N > 0.03\%$  and two seats with a value of  $f_N > 0.10\%$ .

The most important findings when comparing the aerosol distribution in the single-aisle aircraft under MV and CDV conditions are:

- The spread of particles is strongly influenced by the ventilation system: With MV, the aerosol particles are distributed farther in the cabin due to the stronger mixing, which was reflected in many seats with light concentrations (up to 43 seats with  $f_N > 0.03\%$ ) but also up to 16 positions with increased concentrations of  $f_N > 0.10\%$ . CDV, on the other hand, strongly reduces the aerosol spread in the cabin compared to MV, resulting in three seats with  $f_N > 0.10\%$ . Unlike previous studies, no elevated concentrations of CDV were found.
- The mean and maximum aerosol concentration is lower in case of CDV compared to MV conditions.
- The spread of particles in case of MV is strongly influenced by the source position, both longitudinally and in cross-section direction.

Finally, it should be noted that this study does not specify a number of infections during a flight or an infection risk for specific seats. It simply provides a ratio of potentially inhaled aerosols to exhaled aerosols, which can be used as input for determining the risk of infection. In general, lower aerosol exposure also means a lower risk of infection. Here, the reader is referred to, e.g., studies by Webner et al. [[23] who introduced an infection risk model based on direct forward calculation.

### 6. ACKNOWLEDGEMENT

The authors would like to thank Ms. Annika Köhne for proofreading the manuscript.

### 7. REFERENCES

- [1] Lewis, "Mounting evidence suggests coronavirus is airborne but health advice has not caught up," Nature, Vols. https://doi.org/10.1038/d41586-020-02058-1, pp. 510 513, 2020. [Accessed 2nd September 2024].
- [2] WHO, "Transmission of SARS-CoV-2: implications for infection prevention precautions," World Health Organization(WHO), 2021. [Online]. Available: https://www.who.int/newsroom/commentaries/detail/transmission-of-sars-cov-2implications-for-infection-prevention-precautions. [Accessed 2nd September 2024].
- [3] W. Nazaroff, "Indoor bioaerosol dynamics," International Journal of Environment and Health, Volume 26, Issue 1, Pages 61-78, 05 December 2014.
- [4] A. Hartmann, J. Lange, H. Rotheudt and M. Kriegel, "Emissionsrate und Partikelgröße von Bioaerosolen beim Atmen, Sprechen und Husten" Technische Universität Berlin, 22 Juni 2020. [Online]. Available: https://api-depositonce.tuberlin.de/server/api/core/bitstreams/445a3ebc-d2ac-42b2.e970.ged248925025/gentent. [Accessed Oth.]
  - 42b2-a879-8ad248825025/content. [Accessed 9th September 2024].
- [5] M. Bielecki, D. Patel, J. Hinkelbein, M. Komorowski, J. Kester, S. Ebrahim, A. Rodriguez-Morales, Z. Memish and P. Schlagenhauf, "Air travel and COVID-19 prevention in the pandemic and peri-pandemic period: A narrative review," *Travel Medicine ans Infectous Diease*, pp. Volume 39, 101915 https://doi.org/10.1016/j.tmaid.2020.101915, January-February 2021.
- [6] D. Freedman and A. Wilder-Smith, "In-flight transmission of SARS-CoV-2: a review of the attack rates and available data on the efficacy of face masks," *Journal of Travel Medicine*, pp. Volume 27, Issue 8, taaa 178, https://doi.org/10.1093/jtm/taaa178, 25 September 2020.
- [7] R. You, C.-H. Lin, D. Wei and Q. Chen, "Evaluating the commercial airliner cabin environment with different air distribution systems," *International Jurnal of Indoor Environment and Health*, pp. Volume 29, Issue 5, Pages 840-853, https://onlinelibrary.wiley.com/doi/10.1111/ina.12578, September 2019.
- [8] K. Talaat, M. Abuhegazy, O. Mahfoze, O. Anderoglu and S. Poroseva, "Simulation of aerosol transmission on a Boeing 737airplane with intervention measures for COVID-19 mitigation," *Physics for Fluids*, vol. Volume 33, no. Issue 3, p. 033312, 2021.
- [9] P. Lange, T. Dehne, D. Schmeling, A. Dannhauer and I. Gores, "Realistic flight conditions on ground: new

- research facility for cabin ventilation," CEAS Aeronautic Journal, 2022.
- [10] T. Dehne, P. Lange, D. Schmeling and I. Gores, "Micro-Jet Ventilation – a Novel Ventilation Concept for long-range Aircraft Cabins," Ventilation 2022: 13th International Industrial Ventilation Conference for Contaminant Control, Toronto, Canada, 2022.
- [11] T. Dehne, P. Lange, D. Schmeling and I. Gores, "Impact of Non-Occupied Seats on the Thermal Comfort in Long-Range Aircraft for Novel Ventilation Concepts," 17th International Conference on Indoor Air Quality and Climate, Indoor Air 2022; Kuopio, Finland, 2022.
- [12] J. Bosbach, A. Heider, T. Dehne, M. Markwart, I. Gores and P. Bendfeldt, "Evaluation of Cabin Displacement Ventilation under Flight Conditions," in 28th International Congress of the Aeronautical Sciences ICAS2012, Brisbane, Australia, 2012.
- [13] D. Müller, M. Schmidt and B. Müller, "Application of displacement ventilation systems for air flow distribution in aircraft cabins," 3rd International Workshop on Aircraft System Technologies, Hamburg, Germany, 2011.
- [14] T. Zhang and C. Q., "Novel air distribution systems for commercial aircraft cabins," *Building and Environment*, vol. 42, no. 4, pp. 1675 - 1684, 2077.
- [15] J. Bosbach, S. Lange, T. Dehne, G. Lauenroth, F. Hesselbach and M. Allzeit, "Alternative Ventilation Concepts for Aircraft Cabins," CEAS Aeronautic Journal 4, pp. 301 - 313, 2013.
- [16] T. Dehne, J. Bosbach and A. Heider, "Comparison of Surface Temperatures and Cooling Rates for Different Ventilation Concepts in an A320 Aircraft Cabin under Flight Conditions," in 13th SCANVAC International Conference on Air Distribution in Rooms and Airplanes, Sao Pauo, Brazil, 2014.
- [17] T. Dehne, A. Volkmann, D. Schmeling, "Experimental Study of Aerosol Dispersion in a long-range Aircraft Cabin Mock-up", Aircraft Cabin Air Conference, London, England, 2023
- [18] D. Schmeling, T. Dehne, S. Lange, D. Schiepel, A. Shishkin, "Passenger Aircraft Cabin ventilation Investigations within the Do728 Research Facility", AIAA Aviation Forum, San Diego, USA, 2023.
- [19] D. Schmeling, A. Shishkin, D. Schiepel and C. Wagner, "Numerical and experimental study of aerosol dispersion in the Do728 aircraft cabin," CEAS Aeronautical Journal, 2023.
- [20] Bundesvereinigung Deutscher Apotheker-verbände, editor. Deutscher Arzneimittel-Codex®/Neues Rezeptur-Formularium® (DAC/NRF). Eschborn: AVOXA-Mediengruppe Deutscher Apotheker GmbH (2017) (in German).
- [21] Sensirion AG The sensor company, "Sensor for HVAC and air quality applications SPS30", [Online].Available:https://sensirion.com/media/documents/B7AAA101/61653FB8/Sensirion\_Particulate\_Matter\_AppNotes\_Specification\_Statement.pdf [Accessed 16th September 2024].
- [22] Y. Han, Y. Zhang, Y. Gao, X. Hu and Z. Guo, "Vortex structures of longitudinal csale flow in a 28-row aircraft cabin," *Buildind and Environment*, vol. 222, 109362, 2022.
- [23] F. Webner, A. Shishkin, D. Schmeling, C. Wagner, "A Direct Infection Risk Model for CFD Predictions and Its Application to SARS-CoV-2 Aircraft Cabin Transmission", *Indoor Air 2025*, Honolulu, USA, 2024

©2024

8